Composition design for Laves phase-related body-centered cubic–V solid solution alloys with large hydrogen storage capacities

2008 J. Phys.: Condens. Matter 20 114110

(http://iopscience.iop.org/0953-8984/20/11/114110)

J. Phys.: Condens. Matter **20** (2008) 114110 (5pp) doi:10.1088/0953-8984/20/11/114110

Composition design for Laves phase-related body-centered cubic–V solid solution alloys with large hydrogen storage capacities

H B Wang[1], Q Wang[1], C Dong[1], L Yuan[1], F Xu[2] and L X Sun[2]

[1] State Key Laboratory of Materials Modification, Dalian University of Technology, Dalian 116024, People's Republic of China
[2] Materials and Thermochemistry Laboratory, Dalian Institute of Chemical Physics, Chinese Academy of Sciences, Dalian 116024, People's Republic of China

E-mail: wangq@dlut.edu.cn

Received 30 August 2007, in final form 15 November 2007
Published 20 February 2008
Online at stacks.iop.org/JPhysCM/20/114110

Abstract
This paper analyzes the characteristics of alloy compositions with large hydrogen storage capacities in Laves phase-related body-centered cubic (bcc) solid solution alloy systems using the cluster line approach. Since a dense-packed icosahedral cluster A_6B_7 characterizes the local structure of AB_2 Laves phases, in an A–B–C ternary system, such as Ti–Cr (Mn, Fe)–V, where A–B forms AB_2 Laves phases while A–C and B–C tend to form solid solutions, a cluster line A_6B_7–C is constructed by linking A_6B_7 to C. The alloy compositions with large hydrogen storage capacities are generally located near this line and are approximately expressed with the cluster-plus-glue-atom model. The cluster line alloys $(Ti_6Cr_7)_{100-x}V_x$ ($x = 2.5$–70 at.%) exhibit different structures and hence different hydrogen storage capacities with increasing V content. The alloys $(Ti_6Cr_7)_{95}V_5$ and $Ti_{30}Cr_{40}V_{30}$ with bcc solid solution structure satisfy the cluster-plus-glue-atom model.

1. Introduction

Hydrogen storage (H-storage) alloys have been enthusiastically investigated for fuel cell and many other applications [1–3]. The Lave phase-related V-based bcc solid solution alloys [4–10], like Ti–Cr–V, Ti–Fe–V, Ti–Mn–V and Ti–Cr–Mn–V, have been developed rapidly as a new generation of H-storage alloys due to their large H-storage capacities and favorable kinetic characteristics for hydrogen absorption and desorption. However, it is difficult to determine the optimum alloy composition with large H-storage capacity in multi-component alloy systems where large H-storage capacities are generally achieved by multiple alloying of simple binary alloys with tedious trial-and-error methods. Therefore, composition design is of great importance for developing new complex alloys with large H-storage capacities.

The AB_2 Laves phases, including three types of crystalline phase: cF24-$MgCu_2$, hP12-$MgZn_2$ and hP24-$MgNi_2$, are common topologically close-packed structures [11]. We analyzed the local structures of these Laves phases and found that they contain a dense-packed icosahedral cluster A_6B_7 centered with a smaller B atom. Taking the $MgCu_2$ phase for instance, figure 1 gives the unit cell of this phase where a Cu-centered icosahedral cluster Mg_6Cu_7 is identified. From the viewpoint of atomic clusters, it is easy to understand that the $MgCu_2$ phase composition can be decomposed into one Mg_6Cu_7 cluster plus five Cu atoms, i.e. $Mg_6Cu_7 + 5Cu = Mg_6Cu_{12} = MgCu_2$. If the five atoms are regarded as the pseudo-third element, then the straight composition line can be defined by linking the icosahedral Mg_6Cu_7 cluster composition with Cu in a pseudo-ternary Mg–Cu–Cu system, as shown in figure 1. Such a cluster line refers to a straight composition line in a ternary system linking a binary topologically dense-packed cluster to the third element. In other words, this is a cluster-plus-glue-atom model where the third element serves as glue atoms linking atomic clusters. As a practical

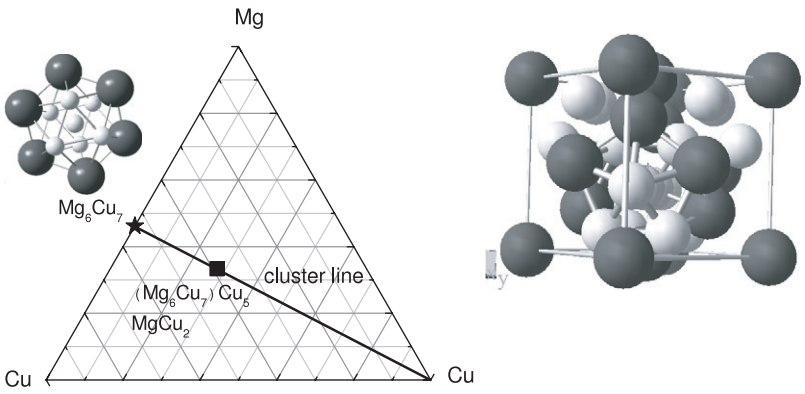

Figure 1. Schematic composition chart of the pseudo-ternary Mg–Cu–Cu system and an $MgCu_2$ unit cell structure where the icosahedron Mg_6Cu_7 is derived.

approach for composition design, the cluster line has guided successfully the composition analysis of quasicrystals and bulk metallic glasses [12–14], where often the local structures exhibit icosahedral short-range order.

The formation of atomic clusters is originated from the negative enthalpy of mixing of constituent elements; thus both the cluster line rule and the cluster-plus-glue-atom model should be general phenomena in other types of alloy phase as well. Therefore, in the present paper, we attempt to analyze the composition characteristics of alloys with large H-storage capacities in the Laves phase-related bcc–V solid solution alloy systems by using the cluster line approach, and to investigate H-storage capacities of cluster line alloys in the Ti–Cr–V ternary system.

2. Cluster line phenomenon in typical bcc–V solid solution alloy systems

2.1. Ti–Cr–V ternary system

The Ti–Cr–V ternary system is a typical bcc solid solution-forming system [5, 6]. The enthalpies of mixing between constituent elements are respectively $\Delta H_{\mathrm{Ti-Cr}} = -7.5$ kJ mol^{-1}, $\Delta H_{\mathrm{Cr-V}} = -2$ kJ mol^{-1}, $\Delta H_{\mathrm{V-Ti}} = -2$ kJ mol^{-1} [15]. So binary Ti–V and Cr–V are solid solution-forming systems while Ti–Cr forms $TiCr_2$ Laves phases of the cF-$MgCu_2$ type (low temperature) and the hP-$MgNi_2$ type (high temperature). The Cr-centered icosahedral Ti_6Cr_7 cluster exemplifies the local structure of the $TiCr_2$ Laves phase. According to the topologically efficient cluster packing structural model [16], the critical ratio R^* of the ideally dense-packed icosahedral cluster is 0.902, which is defined as the ratio of the radius of the center atom r_0 to that of the nearest-neighbor shell atom r_1. Here, the Goldschmidt radii of Cr and Ti atoms are respectively 0.128 nm and 0.146 nm, and then the ratio R of the Ti_6Cr_7 cluster is $R = r_0/r_1 = 0.128/[(0.128 \times 6 + 0.146 \times 6)/12] = 0.934$, where r_1 is the average atomic radius of the nearest-neighbor shell atoms Cr_6Ti_6. The difference represented by $\Delta = (R - R^*)/R^*$ between the actual R and the ideal R^* is 3.5%, which indicates that the icosahedral cluster Ti_6Cr_7 is quite densely packed.

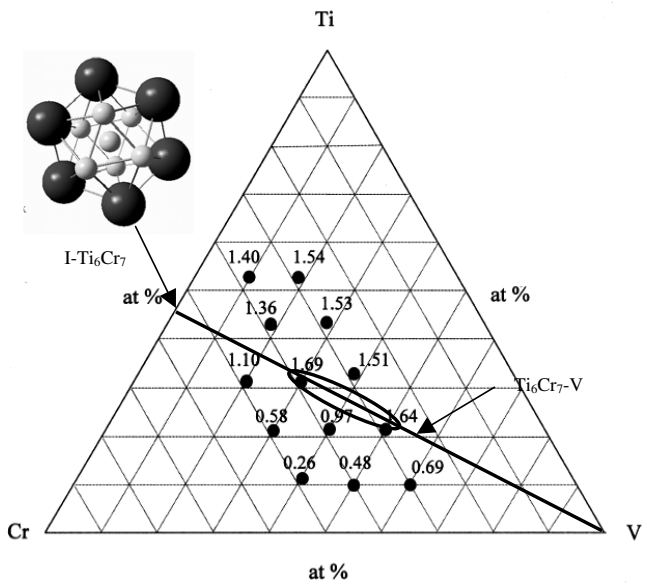

Figure 2. Composition chart of the Ti–Cr–V ternary system. The cluster line Ti_6Cr_7–V is plotted and the H-storage capacities (H/M) of some Ti–Cr–V alloys at 303 K [5] are also listed.

Thus the cluster line Ti_6Cr_7–V is constructed in the Ti–Cr–V ternary system by linking the binary cluster Ti_6Cr_7 with V as shown in figure 2. In figure 2, the black circles and neighboring numbers represent the Ti–Cr–V alloy compositions and the H-storage capacities (H/M) of the designed alloys, respectively [5]. It is noted that the icosahedral cluster line Ti_6Cr_7–V traverses exactly the composition range with large H-storage capacities, which verifies the validity of the cluster line approach for the Ti–Cr–V H-storage alloy system. Furthermore, the best experimental alloy composition $Ti_{30}Cr_{40}V_{30}$ with the largest H-storage capacity (H/M = 1.69) is approximately expressed with the cluster-plus-glue-atom model of $(Ti_6Cr_7)_1V_5$ ($=Ti_{33.3}Cr_{38.9}V_{27.8}$), i.e. one Ti_6Cr_7 cluster glued with five V atoms, where the number of glue atoms V is the same as that of glue atoms Cu in the $MgCu_2$ Laves phase.

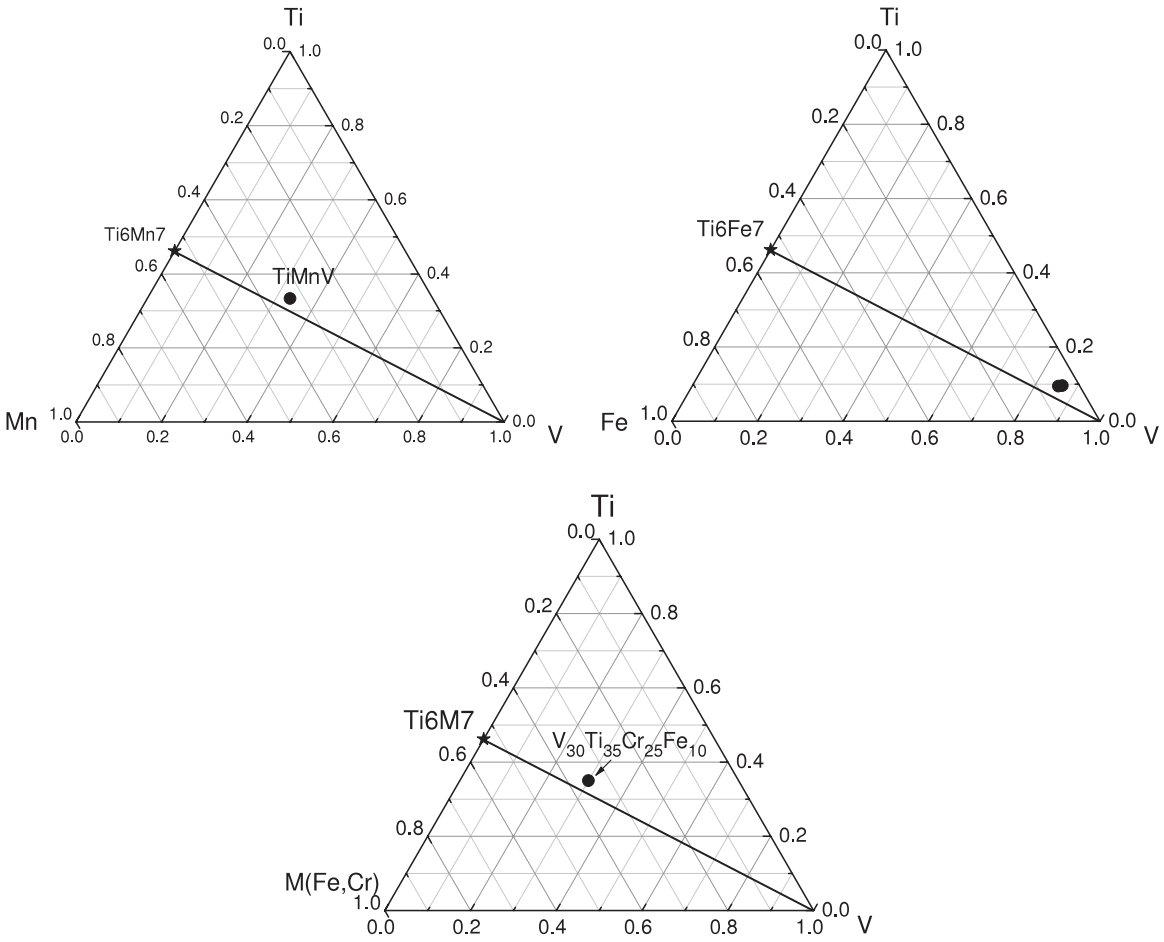

Figure 3. Composition charts of Ti–Mn–V, Ti–Fe–V and Ti–(Cr, Fe)–V ternary systems.

2.2. Ti–Mn–V ternary system

The cluster line approach for this ternary system is similar to that for the Ti–Cr–V system. The Ti–Mn and Mn–V enthalpies of mixing are respectively $\Delta H_{\mathrm{Ti-Mn}} = -8$ kJ mol^{-1}, $\Delta H_{\mathrm{Mn-V}} = -0.8$ kJ mol^{-1} [15]. Therefore Ti and Mn tend to form the $TiMn_2$ Laves phase while V forms solid solutions both with Ti and Mn. The $TiMn_2$ Laves phase has an hP-$MgZn_2$ structure and is characterized by the Mn-centered dense-packed icosahedral cluster Ti_6Mn_7 ($\Delta = 2.7\%$, $r_{\mathrm{Mn}} = 0.126$ nm). The cluster line Ti_6Mn_7–V is then constructed in the Ti–Mn–V system as shown in figure 3. Experimental results indicate that the TiMnV alloy consisting of ternary Laves alloy distributed in a bcc–V solid solution matrix has a large H-storage capacity [9]. It can be seen from figure 3 that this ternary alloy is located near the cluster line Ti_6Mn_7–V and also close to the $(Ti_6Cr_7)_1V_5$ composition, indicating that the alloys near the cluster line may have large H-storage capacities.

2.3. Ti–Fe–V ternary system

The large Ti–Fe and Fe–V enthalpies of mixing ($\Delta H_{\mathrm{Ti-Fe}} = -17$ kJ mol^{-1}, $\Delta H_{\mathrm{Fe-V}} = -8$ kJ mol^{-1}) favor the formation of intermetallics. Similarly, the Fe-centered dense-packed icosahedral cluster Ti_6Fe_7 ($\Delta = 3.1\%$, $r_{\mathrm{Fe}} = 0.127$ nm) exists in the local structure of $MgZn_2$-type $TiFe_2$ Laves phase. In the Ti–Fe–V ternary system, the V-rich alloy compositions with large H-storage capacities [8] (represented by full-circle points in figure 3) are also located near the cluster line Ti_6Fe_7–V.

2.4. Ti–Cr–Fe(Mn)–V quaternary systems

In Ti–Cr–Fe–V and Ti–Cr–Mn–V quaternary systems, Cr–Fe and Cr–Mn can be regarded as a pseudoelement M due to their similar atomic radii and similar enthalpies of mixing with Ti or V. Thus, the quaternary Ti–Cr–Fe–V alloy composition $Ti_{35}Cr_{25}Fe_{10}V_{30}$ [17] with a large H-storage capacity can be expressed as a pseudo-ternary composition $Ti_{35}M_{35}V_{30}$, which is located near the icosahedral cluster line Ti_6M_7–V in the pseudo-ternary alloy system (see in figure 3) and also close to the $(Ti_6M_7)_1V_5$ composition.

A general characteristic for the above Laves phase-related bcc–V solid solution alloy systems A–B–C is that the absolute value of $\Delta H_{\mathrm{A-B}}$ is larger than $\Delta H_{\mathrm{B-C}}$ and $\Delta H_{\mathrm{A-C}}$ and the latter two are close to zero. A–B then forms an AB_2 Laves phase while A–C and B–C tend to form solid solutions. Thus, the dense-packed icosahedral cluster line A_6B_7–C can be applied to these ternary and pseudo-ternary systems and alloy compositions with large H-storage capacities are located near the cluster line.

In the present work, the Ti–Cr–V alloy compositions are designed along the icosahedral cluster line Cr_7Ti_6–V

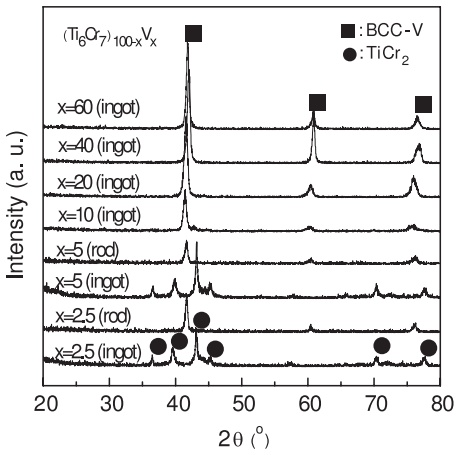

Figure 4. XRD patterns of the $(Ti_6Cr_7)_{100-x}V_x$ (x = 2.5–70 at.%) cast alloy ingots and suction-cast rods.

and the H-storage capacities of these cluster line alloys are investigated.

3. Experimental details

Ingots of the $(Ti_6Cr_7)_{100-x}V_x$ (x = 2.5–70 at.%) alloys were prepared by arc melting the mixtures of constituent elements under argon atmosphere. The purities of the elements are 99.9 wt% for Cr, 99.99 wt% for Ti and 99.5 wt% for V, respectively. Alloy rods with a diameter of 3 mm were prepared by means of copper mold suction casting. Structural identification of these alloys was carried out by means of x-ray diffractometry (XRD) with Cu Kα radiation (λ = 0.154 06 nm). The alloy ingots and rods were mechanically crushed into powders under 300 μm. The activation treatment was carried out as follows. The sample powders, about 2 g, were put into the reactor and evacuated for 30 min at 673 K. The hydrogen with a pressure of 5 MPa was introduced into the reactor for 30 min. The reactor was subsequently quenched in water and was again evacuated for 30 min at 673 K. This processing is repeated 3–4 times. Finally, the P–C isotherms (PCT curves) for the samples were measured at 288 and 313 K under a hydrogen pressure of 5 MPa.

4. Results and discussion

Figure 4 shows the XRD results for the cast $(Ti_6Cr_7)_{100-x}V_x$ (x = 2.5–70 at.%) alloy ingots and rods. For the alloy ingots at V contents x = 2.5 and 5 at.%, the Cr_2Ti phase is formed; with increasing V content, dual-phase $TiCr_2$–bcc solid solutions appear in the range of x = 10–20 at.%; then upon further increasing the V content, only bcc solid solution phase is maintained in the range of x = 20–70 at.%, while for the alloy rods prepared by suction casting with x = 2.5 and 5 at.%, the $TiCr_2$ phase is absent and is replaced by a single bcc structure. Note that only the cluster line alloys of x = 2.5 and 5 at.% can be suction cast as rods.

The H-storage capacities of the cluster line alloys vary with temperature. Figures 5(a) and (b) show the PCT curves of four typical cast $(Ti_6Cr_7)_{100-x}V_x$ (x = 2.5, 10, 40, 60 at.%) alloy ingots at different temperatures. At 288 K (figure 5(a)), the hydrogen absorbing capacity of the alloy x = 2.5 at.% containing the pure $TiCr_2$ phase is weak and no plateau appears in the PCT curve. With increased V content, the hydrogen absorbing capacities of the bcc solid solution alloys along the cluster line are enhanced and the alloys x = 40 and 60 at.% can absorb at maximum about 2.5 wt% of hydrogen, while the H-storage capacities at a higher temperature of 313 K are larger (figure 5(b)). The maximum hydrogen contents of these alloys are all larger than 3 wt%. Although the alloy $(Ti_6Cr_7)_{90}V_{10}$ absorbs 3.32 wt% of hydrogen, the PCT curve is steep and the effective H-storage capacity is weak. The bcc solid solution alloy x = 40 at.% has the largest effective hydrogen storage capacity and can absorb about 3.19 wt% of hydrogen, which is consistent with the value reported in the literature [5].

For the same composition, the H-storage capacity varies with the alloy structure. As shown in figure 5(c), the H-absorbing contents of the alloy rods are larger than those of the alloy ingots. Taking $(Ti_6Cr_7)_{95}V_5$ for instance, the maximum H-absorbing content of the alloy ingot with pure $TiCr_2$ phase reaches 1.8 wt%, while the alloy rod with bcc–V solid solution structure can absorb at most 3.14 wt% of hydrogen. Furthermore, the H-absorbing capacity of this alloy in both ingot and rod forms is larger than that of the $(Ti_6Cr_7)_{97.5}V_{2.5}$ alloys. The hydrogen absorption and desorption capacities of the $(Ti_6Cr_7)_{95}V_5$ alloy rod are comparable to those of $(Ti_6Cr_7)_{60}V_{40}$ alloy ingot. Although the two alloys possess bcc–V solid solution structure, the former contains much less V content, which reduces the material cost.

From the viewpoint of the cluster-plus-glue-atom model, the alloy composition $(Ti_6Cr_7)_{95}V_5$ ($Ti_{43.8}Cr_{51.2}V_5$) with large H-storage capacity is approximately expressed as $(Ti_6Cr_7)_1V_1$ (=$Ti_{42.9}Cr_{50}V_{7.1}$), which is consistent with those optimum quasicrystals and bulk metallic glasses also determined by the $(\text{cluster})_1(\text{glue atom})_1$ model [12–14]. This is supported by the efficient cluster packing model proposed by Miracle [18]: dense-packed clusters centered with primary solute atoms are packed in a close-packed face-centered cubic (fcc) like structure and the secondary solute atoms (or glue atoms as we call them) are located in the interstitial sites. An fcc unit cell includes four lattice sites, four octahedral interstices and eight tetrahedral interstices. Thus the ratio of the number of atoms to that of octahedral and tetrahedral interstices is 1:3. The ratio 1:1 for the number of clusters to that of glue atoms indicates that glue atoms only occupy the octahedral interstices, while the ratio 1:3 indicates that the glue atoms take up all the octahedral and tetrahedral interstices. Ma *et al* [19] further revised the efficient cluster packing model and pointed out that double atoms can fill into interstitial sites. If double atoms fill into an octahedral interstice, the ratio of the number of clusters to that of glue atoms will be 1:5, which is consistent with cluster-plus-glue-atom expression for the Laves phase and V solid solution alloys with large H-storage capacities.

5. Conclusions

The hydrogen storage characteristics of ternary Laves phase-related bcc solid solution alloys Ti–(Cr, Mn, Fe)–V have been analyzed by using the cluster line approach. It is revealed that the alloy compositions with large hydrogen

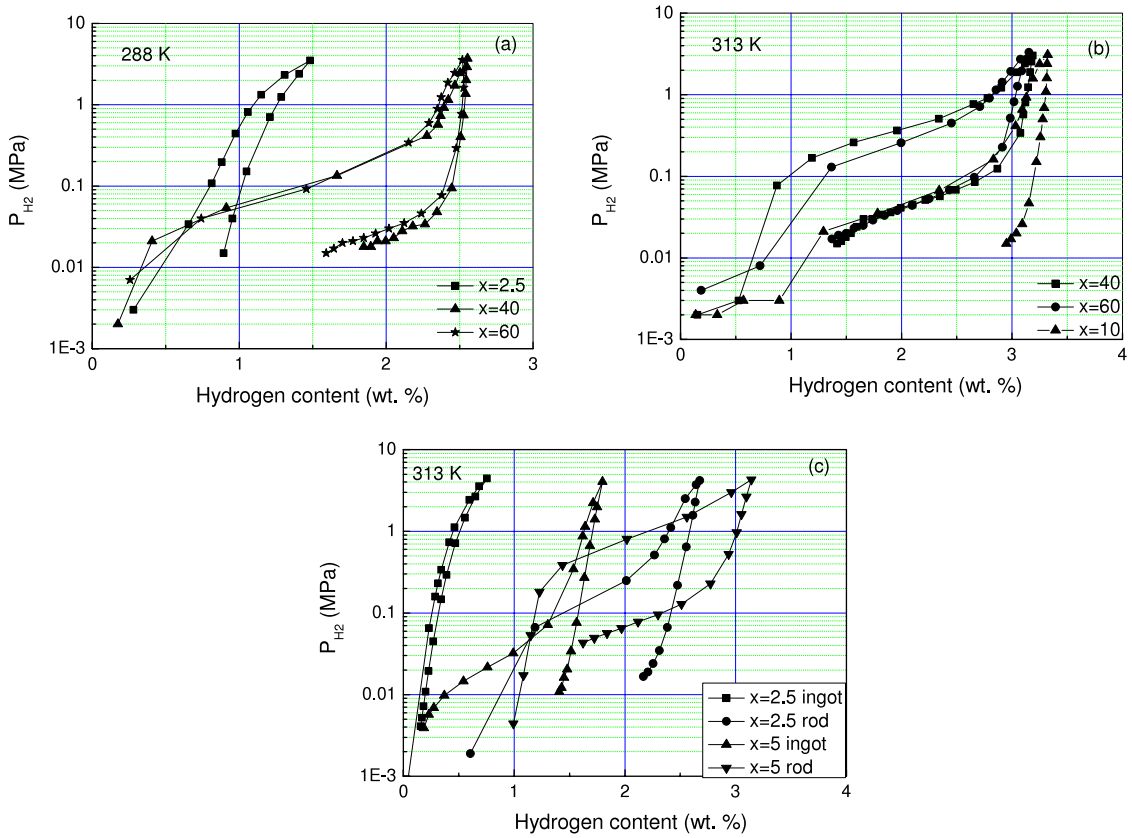

Figure 5. *PCT* curves of the $(Ti_6Cr_7)_{100-x}V_x$ ($x = 2.5$–60 at.%) alloy ingots and rods (after copper mold suction casting, with a 3 mm diameter).

(This figure is in colour only in the electronic version)

capacities are located near the dense-packed icosahedral cluster line $Ti_6(Cr, Mn, Fe)_7$–V. In the Ti–Cr–V ternary system, the structures of the cluster line $(Ti_6Cr_7)_{100-x}V_x$ ($x = 2.5$–70 at.%) alloy ingots prepared by conventional casting evolve with increasing V content from pure Laves phase, then to dual-phase $TiCr_2$–bcc solid solution structures, and finally to the bcc solid solution. Upon suction casting, the alloy rods all contain a single bcc solid solution. Among these, the $(Ti_6Cr_7)_{95}V_5$ bcc alloy after suction casting exhibits a high hydrogen storage capacity of 3.14 wt%, which is comparable with that of the best known alloy, V-rich $Ti_{30}Cr_{40}V_{30}$ prepared by conventional casting. Moreover, these two alloy compositions can be expressed according to the cluster-plus-glue-atom model as $(Ti_6Cr_7)_{95}V_5 \approx (Ti_6Cr_7)_1V_1$ and $Ti_{30}Cr_{40}V_{30} \approx (Ti_6Cr_7)_1V_5$.

Acknowledgments

This project was supported by the National Science Foundation of China (Nos 50631010, 50671018 and 10774019) and the National Basic Research Program of China (No. 2007CB613902).

References

[1] Libowitz G G and Maeland A 1988 *Mater. Sci. Forum* **30** 177
[2] Maeland A J, Libowitz G G, Lynch J F and Rak G J 1984 *J. Less-Common Met.* **104** 133
[3] Maeland A J, Libowitz G G and Lynch J F 1984 *J. Less-Common Met.* **104** 361
[4] Akiba E and Iba H 1998 *Intermetallics* **6** 461
[5] Cho S W, Han C S, Park C N and Akiba E 1999 *J. Alloys Compounds* **288** 294
[6] Tamura T, Kazumi T, Kamegawa A, Takamura H and Okada M 2003 *J. Alloys Compounds* **356/357** 505
[7] Lynch J F, Maeland A J and Libowitz G G 1985 *Z. Phys. Chem. NF* **145** 51
[8] Nomura K and Akiba E 1995 *J. Alloys Compounds* **231** 513
[9] Iba H and Akiba E 1997 *J. Alloys Compounds* **253/254** 21
[10] Tamura T, Tominaga Y, Matsumoto K, Fuda T, Kuriiwa T, Kamegawa A, Takamura H and Okada M 2002 *J. Alloys Compounds* **330–332** 522
[11] Massalski T B 1983 *Physical Metallurgy Part I* (New York: North-Holland) p 190
[12] Xia J H, Qiang J B, Wang Y M, Wang Q and Dong C 2006 *Appl. Phys. Lett.* **88** 101907
[13] Yang L, Xia J H, Wang Q, Dong C, Chen L Y, Ou X, Liu J F, Jiang J Z, Klementiev K, Saksl K, Franz H, Schneider J R and Gerward L 2006 *Appl. Phys. Lett.* **88** 241913
[14] Dong C, Wang Q, Qiang J B, Wang Y M, Jiang N, Han G, Li Y H and Wu J 2007 *J. Phys. D: Appl. Phys.* **40** R1
[15] de Boer F R and Pettifor D G 1989 *Cohesion in Metals and Transition Metal Alloys* (Amsterdam: North-Holland) p 167
[16] Miracle D B and Sanders W S 2003 *Phil. Mag.* **83** 2409
[17] Yan Y G, Chen Y G, Liang H, Liang J and Wu C L 2006 *Rare Metal Mater. Eng.* **35** 686
[18] Miracle D B 2006 *Acta Mater.* **54** 4317
[19] Wang A P, Wang J Q and Ma E 2007 *Appl. Phys. Lett.* **90** 121912